01 Sep 2006

Microbial Growth and Biofilm Formation in Geologic Media Is Detected with Complex Conductivity Measurements

Caroline A. Davis

Estella A. Atekwana
Missouri University of Science and Technology, atekwana@mst.edu

Eliot A. Atekwana
Missouri University of Science and Technology

Lee D. Slater

et. al. For a complete list of authors, see https://scholarsmine.mst.edu/geosci_geo_peteng_facwork/88

Microbial growth and biofilm formation in geologic media is detected with complex conductivity measurements

Caroline A. Davis,[1] Estella Atekwana,[2] Eliot Atekwana,[2] Lee D. Slater,[3] Silvia Rossbach,[4] and Melanie R. Mormile[5]

[1] Complex conductivity measurements (0.1–1000 Hz) were obtained from biostimulated sand-packed columns to investigate the effect of microbial growth and biofilm formation on the electrical properties of porous media. Microbial growth was verified by direct microbial counts, pH measurements, and environmental scanning electron microscope imaging. Peaks in imaginary (interfacial) conductivity in the biostimulated columns were coincident with peaks in the microbial cell concentrations extracted from sands. However, the real conductivity component showed no discernible relationship to microbial cell concentration. We suggest that the observed dynamic changes in the imaginary conductivity (σ'') arise from the growth and attachment of microbial cells and biofilms to sand surfaces. We conclude that complex conductivity techniques, specifically imaginary conductivity measurements are a proxy indicator for microbial growth and biofilm formation in porous media. Our results have implications for microbial enhanced oil recovery, CO_2 sequestration, bioremediation, and astrobiology studies. **Citation:** Davis, C. A., E. Atekwana, E. Atekwana, L. D. Slater, S. Rossbach, and M. R. Mormile (2006), Microbial growth and biofilm formation in geologic media is detected with complex conductivity measurements, *Geophys. Res. Lett.*, *33*, L18403, doi:10.1029/2006GL027312.

1. Introduction

[2] Several laboratory studies have demonstrated the utility of geophysical methods for the investigation of microbial-induced changes in porous geologic media. The primary suggestion of these studies was that temporal variations in the geophysical signatures corresponded with microbial-induced changes in the geologic media, such as changes in pore fluid chemistry [*Atekwana et al.*, 2004], redox conditions [*Naudet and Revil*, 2005], sulfide mineral precipitation [*Ntarlagiannis et al.*, 2005a; *Williams et al.*, 2005], increase in surface area resulting from attachment of microbes to mineral surfaces [*Abdel Aal et al.*, 2004], or pore clogging due to the presence of microbial cells [*Ntarlagiannis et al.*, 2005b]. Although the above studies have increased our understanding of microbial-induced changes on the geophysical response of geologic media, the direct contribution of microbial growth and biofilm formation on the geophysical response of geologic media remains unknown.

[3] Notable is the use of electrical conductivity in conjunction with other methods (e.g., pH), to detect changes in the chemical properties of pore solutions caused by microbial growth and metabolism in geologic media [e.g., *Silverman and Munoz*, 1974; *Abdel Aal et al.*, 2004]. A laboratory column experiment by *Ntarlagiannis et al.* [2005b] showed a 15% enhanced polarization associated with the direct presence of dormant live (pure culture) bacterial cells in silica sands. *Ntarlagiannis et al.* [2005b] tentatively attributed this polarization enhancement at high cell densities to a combination of decreased ionic mobility and electron transfer associated with cell accumulation in pore throats.

[4] The work described in this letter advances the work of *Ntarlagiannis et al.* [2005b] by using an environmental (mixed) bacterial culture, and allowing for microbial growth and biofilm formation, being more similar to typical field conditions. Understanding the effect of microbial growth and biofilm formation on the geophysical response of geologic media has implications for microbial enhanced oil recovery (MEOR), CO_2 sequestration, and bioremediation investigations, as well as studies focused on the development of techniques for the detection of extraterrestrial life. Here we show an apparent correlation between imaginary conductivity and microbial growth, and infer that imaginary conductivity measurements can be used as an indicator of microbial growth and biofilm formation in porous geologic media.

2. Methods

2.1. Experimental Column Setup

[5] The experimental columns used in this study were 30 cm long (Figure 1) and constructed from 3.2 cm inner diameter polyvinyl chloride pipe (PVC). Two Ag-AgCl current injection electrode coils were installed 16 cm apart in the column, and two Ag-AgCl potential electrodes (9 cm apart) were installed between the current electrodes. A fluid reservoir constructed of 7.6 cm PVC pipe was installed on top of each column to allow for fluid sampling. Columns were dry-packed with 20–30 mesh silica sand (99.8% silicon dioxide, 0.020% iron oxide, 0.06% aluminum oxide, 0.01% titanium oxide, <0.01% calcium oxide, <0.01% magnesium oxide, <0.01% sodium oxide, <0.01% potassium oxide). The sands were washed with deionized water and

[1]Department of Geological Sciences and Engineering, University of Missouri-Rolla, Rolla, Missouri, USA.
[2]Boone Pickens School of Geology, Oklahoma State University, Stillwater, Oklahoma, USA.
[3]Department of Earth and Environmental Sciences, Rutgers University, Newark, New Jersey, USA.
[4]Department of Biological Sciences, Western Michigan University, Kalamazoo, Michigan, USA.
[5]Department of Biological Sciences, University of Missouri-Rolla, Rolla, Missouri, USA.
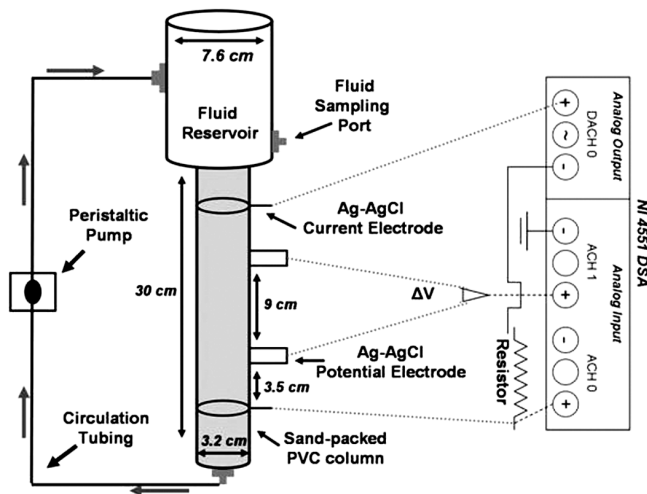
Figure 1. Schematic diagram showing the experimental set up. A digital signal analyzer (DSA) was used to collect the low frequency electrical measurements.

disinfected by autoclaving prior to being packed in the columns. All columns, tubing, and accessories were disinfected by rinsing with 70% ethanol.

[6] Two sets of electrical columns were constructed in duplicate, and a third column was constructed for solid phase analysis. One set was used for unstimulated (background) measurements (nutrients + diesel fuel) and one set for biostimulated (experimental) measurements (nutrients + diesel fuel + bacterial culture). Columns were saturated with a sterile 25% Bushnell Haas (BH) nutrient broth (Becton Dickinson; 50 mg/l magnesium sulfate, 5 mg/l calcium chloride, 250 mg/l monopotassium phosphate, 250 mg/l diammonium hydrogen phosphate, 250 mg/l potassium nitrate, 12.5 mg/l ferric chloride), diesel fuel, and the biostimulated columns were amended with a mixed bacterial culture that was cultured from sediments collected at a hydrocarbon contaminated site in Carson City, MI, USA. The mixed culture is known to contain hydrocarbon degraders such as strains of *Variovorax* and *Stenotrophomonas*. The fluid in each column was circulated for 30 min by using a peristaltic pump prior to electrical measurements, fluid sampling, and sand sampling.

2.2. Complex Conductivity Measurements

[7] Complex conductivity measurements (0.1–1000 Hz) were obtained by using a four-electrode technique (Figure 1) based around a National Instruments (NI) 4551 dynamic signal analyzer [*Vanhala and Soininen*, 1995; *Slater and Lesmes*, 2002]. The impedance magnitude $|\sigma|$ and the phase shift ϕ (between a measured voltage sinusoid and an impressed current sinusoid) of the sample were measured relative to a high-quality resistor. The real ($\sigma' = |\sigma| \cos \phi$) and imaginary ($\sigma'' = |\sigma| \sin \phi$) parts of the sample complex conductivity were then calculated. The electrical measurements were made twice a week for the 60 day duration of the experiment. Experimental uncertainty in the electrical measurements was calculated by averaging the electrical data for duplicate columns, and calculating the standard deviation from the average.

2.3. Sampling and Analyses

[8] Fluid conductivity (σ_w) and pH were measured using microelectrodes immediately after fluids were withdrawn from the fluid reservoirs at the top of the columns. BH broth was periodically added (day 18, and 31) to the fluid reservoir to maintain the fluid volume in the reservoir. Experimental uncertainty in the geochemical measurements was calculated by averaging the geochemical data for duplicate columns, and calculating the standard deviation from the average.

[9] Sand samples were collected from the sand sampling columns beginning on day 13 of the experiment, immediately after fluid samples were collected. The sand samples were used for (1) extraction of bacterial cells for direct microbial counts, and (2) environmental scanning electron microscope (ESEM) imaging of grain surface characteristics. Live and dead microbial cell numbers were determined by direct counting using an epifluorescent microscope [*Bunthof et al.*, 2001]. Bacterial cells were extracted from 0.5g of wet sand using an extraction technique modified after *Lehman et al.* [2001]. After extraction, the bacterial cells were washed with 0.85% NaCl solution, stained, and prepared for direct counts using a Live/Dead BacLight Bacterial Viability Kit. The average live cell concentrations and average dead cell concentrations were calculated, and experimental uncertainty was determined by calculating the standard deviation from the average of duplicate counts.

[10] A portion of the sand samples collected from the columns were imaged using an ESEM. Images of the sand surface characteristics and attached microbial cells and biofilms were obtained by Hitachi High Technologies America, Inc. using a Hitachi S3400 ESEM fitted with secondary and backscattered electron detectors. The ESEM operating parameters varied depending on the surface characteristic being imaged, and ranged from 2.5–8.0 kV, 5.9–11.1 mm, 700x–3000x, for accelerating voltage, working distance, and magnification, respectively.

3. Results

3.1. Complex Conductivity

[11] The complex conductivity measurements were corrected for changes in temperature effects using correction equation y = 0.0003x + 0.0084 (R^2 = 0.99) and y = 0.0000001x + 0.000002 (R^2 = 0.98) at 25C, for the real and imaginary conductivity, respectively. Temperature correction equations were determined from laboratory experiments designed to measure the effect of temperature variations on the complex conductivity measurements. Fluid conductivity values were automatically corrected for changes in temperature by the conductivity microelectrode.

[12] The complex conductivity measurements are shown in Figures 2a and 2b. We show the electrical data at 2 Hz, as this frequency is close to typical frequencies used in field electrical measurements. This was also the frequency at which our measurement error was lowest. The σ'' in the biostimulated columns increased by ~280% from ~2.0 × 10^{-6} S/m on day 0 to peak values (~7.8 × 10^{-6} S/m) between day 18 and 23, before steadily decreasing to ~2.0 × 10^{-6} S/m on day 40. The magnitude of the σ'' response in the unstimulated columns was relatively small
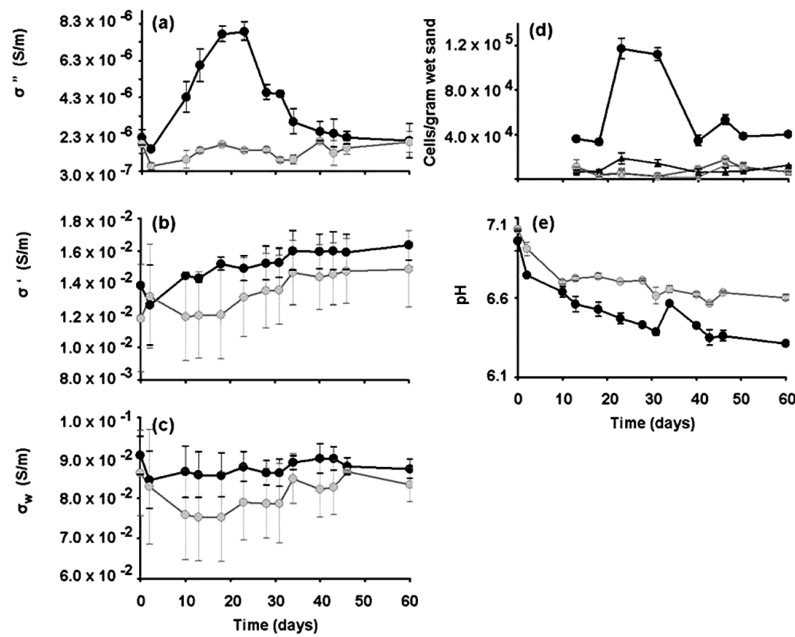
Figure 2. Results of the measured (a) σ'', (b) σ', (c) σ_w, (d) microbial cell concentrations, and (e) pH. In Figures 2a, 2b, 2c, and 2e closed black circles represent biostimulated column measurements, and closed gray symbols represent unstimulated column measurements. Microbial cell concentrations (Figure 2d) are shown as biostimulated column live cells (black closed circle), unstimulated live cells (gray closed circles), biostimulated column dead cells (black closed triangle), and unstimulated column dead cells (gray closed triangle). Error bars represent measurement uncertainty reported as standard deviation from average of duplicate measurements.

compared to the biostimulated columns, increasing slightly and varying by $\sim 1.5 \times 10^{-7}$ S/m over the duration of the experiment and rarely exceeding the initial values at the start of the experiment. The σ' (Figure 2b, showed a relatively steady increase over the duration of the experiment for both the unstimulated (up to $\sim 1.5 \times 10^{-2}$ S/m or $\sim 28\%$ increase) and biostimulated (up to $\sim 1.6 \times 10^{-2}$ S/m or $\sim 18\%$ increase) columns. The σ_w (Figure 2c) of the biostimulated columns decreased slightly for the first few days (by $\sim 5\%$) to $\sim 8.0 \times 10^{-2}$ S/m, before increasing slightly for the rest of the experiment. The σ_w of the unstimulated columns varied to a greater degree ($\sim 12\%$) than the biostimulated columns, decreasing for the first 20 days by $\sim 12\%$ to 7.5×10^{-2} S/m, before increasing to $\sim 8.3 \times 10^{-2}$ S/m by day 60.

3.2. Microbial and Geochemical Analyses

[13] Temporal variations in the live and dead microbial cell concentrations (presented as cells/gram of wet sand weight) for both biostimulated and unstimulated columns are shown in Figure 2d. Live cell concentrations in the biostimulated column increased by $\sim 230\%$, from $\sim 3.6 \times 10^4$ cells/g on day 13 to peak concentrations on day 23 ($\sim 1.2 \times 10^5$ cells/g), before declining to $\sim 3.0 \times 10^4$ cells/g on day 40. Although the dead cell concentrations within the biostimulated columns were generally lower than the live cell concentrations, they displayed a similar trend to the live cell concentrations, albeit to a lesser degree. The dead cell concentrations increased from $\sim 4.6 \times 10^3$ cells/g on day 13 to peak concentrations on day 23 ($\sim 1.9 \times 10^4$ cells/g), and decreased to $\sim 6.0 \times 10^3$ cells/g on day 40. The microbial cell concentrations from the unstimulated column initially decreased during the first 30 days of the experiment before

increasing with values varying between $\sim 2 \times 10^3$ cells/g and 2×10^4 cells/g for the duration of the experiment (both live concentrations and dead concentrations). The error associated with the cell concentrations was less than 1.8×10^4 cells/g and 1.5×10^4 cells/g for the biostimulated column live and dead cell concentrations, respectively, and less than 1.2×10^4 cells/g and 1.0×10^4 cells/g for the unstimulated column live and dead cell concentrations, respectively.

[14] A temporal decrease in pH was observed for both the biostimulated and unstimulated columns (Figure 2e). The biostimulated columns showed a relatively greater decrease ($\sim 7 - 6.3$) than the unstimulated columns ($\sim 7 - 6.6$).

3.3. Grain Surface Characteristics

[15] We show four representative ESEM images of surfaces of sand samples obtained on day 23 and day 46 (Figure 3). The images from day 23 of the biostimulated column show a network of extracellular structures between sand grains (Figure 3a), as well as the attachment of individual bacterial cells (Figure 3b) to the sand surfaces. The image from day 23 of the unstimulated column (Figure 3c) shows the relatively smooth, uncolonized surface of a sand grain. Figure 3d shows a backscattered electron composition image of the surface of a sand grain from day 46 of the biostimulated column with features that may represent extracellular or biomat-like structures.

4. Discussion

[16] ESEM images confirm microbial growth and biofilm formation in the biostimulated column. The complex conductivity measurements show that changes in σ'' generally
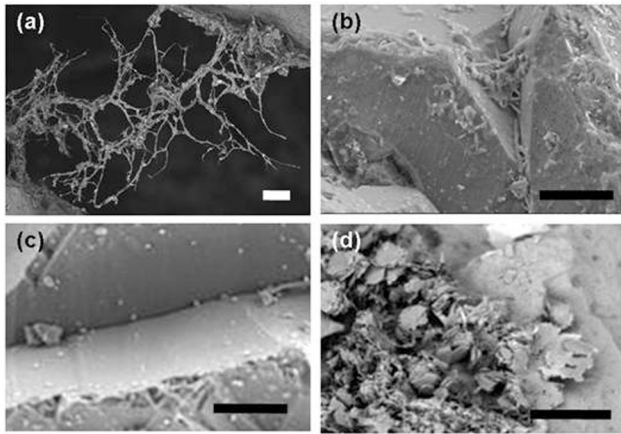
Figure 3. Environmental scanning electron microscope images of sand from (a, b) day 23 of the biostimulated column, (c) day 23 of the unstimulated column, and (d) day 46 of the biostimulated column. Scale bar on each image represents 10 μm.

paralleled those of the microbial counts, with a close correspondence in the peaks and magnitude (up to 280%) of the σ'' and that of the cell concentrations (up to 230%) in the biostimulated columns (Figures 2a and 2d). Since the microbial cell concentrations were measured from microbial cells extracted from sand grains, the close correspondence of the peaks and magnitudes of change of both parameters suggest that the σ'' response resulted directly from the microbial growth and attachment. The unstimulated column, however, did not show any close correspondence between cell concentration and σ''.

[17] From our results, we infer the following: the increase in microbial cell concentration (Figure 2d) and σ'' observed in the biostimulated column (day $13-23$) may be in whole or in part due to the increased attachment of cells/biofilms to the surface of sand grains, and/or the increased aggregation of cells into microcolonies [e.g., *Watnick and Kolter*, 2000]. The subsequent decrease in the live microbial cell concentration (day $23-60$), and corresponding decrease in σ'' may be due to an increased rate of detachment [e.g., *Watnick and Kolter*, 2000] or death and lysis of cells [*Mai-Prochnow et al.*, 2004], possibly due to limited nutrients/carbon source or from excessive cell density. The idea of cell death and lysis, the process in which the cell disintegrates and the contents enter the bulk fluid, is a plausible explanation for not observing an increase in the dead cell concentration after day 30.

[18] This suggestion is further supported by the ESEM images of sand from the biostimulated column, which showed high numbers of attached cells and extracellular structures on day 23 (Figure 3a), while less attached biomass is apparent on day 46 (Figure 3d). Whereas *Ntarlagiannis et al.* [2005b] investigated the electrical response of live dormant cells and speculated on the cause of the electrical response, the ESEM images (Figure 3) presented in this study, provides strong evidence to support our findings that the σ'' response is associated with cell aggregation/biofilm formation. The ESEM image from day 23 of the biostimulated column (Figure 3a) showing the extracellular material between sand grains, looks similar to

the conductive extracellular structures known as nanowires that have been found in recent studies [i.e., *Reguera et al.*, 2005; *Gorby et al.*, 2006]. The nanowire structures have been documented to facilitate electron transport from cells to solid phase electron acceptors and typically develop under nutrient (terminal electron acceptor) limiting conditions [*Gorby et al.*, 2006]. Consequently, they may provide the necessary connections needed for charge transfer in microbially active systems and thus be responsible in part for the geoelectrical response observed in biostimulated porous material. However, more laboratory studies are needed to confirm or refute this hypothesis.

[19] A relatively steady temporal increase in the σ' was observed in both the biostimulated and unstimulated columns. We used pure silica sands to minimize weathering in the columns and therefore did not expect to observe any significant changes in σ'. Hence, we are not sure as to the cause for the changes in σ'. However, we speculate that the temporal increase in the σ' may be due to the periodic addition of BH nutrients (Day 18 and 31) to the columns, which would increase the ionic concentration of the pore fluid. This increase in the ionic concentration of the pore fluid is observed in the σ_w, albeit to a lesser magnitude. We note that *Ntarlagiannis et al.* [2005b] also observed changes in the σ' in their experimental columns not explained by the fluid conductivity data.

[20] In conclusion, the results from this study provide evidence that complex conductivity measurements, specifically imaginary conductivity measurements, can be used as a proxy indicator of microbial growth, attachment, and biofilm formation in porous geologic media. We surmise that the observed polarization (σ'') response arises from the direct interaction of the attachment of microbial cells and biofilm development on mineral grain surfaces. These results further our understanding of the direct effect of microbial growth on electrical measurements, and have implications for geoelectrical investigations of environments with enhanced microbial growth/activity. Our work may lead to the application of complex conductivity measurements to field investigations, such as studies aimed at assessing the (1) integrity of subsurface biofilm barriers (biobarriers) used to remediate contaminants or seal reservoirs for CO_2 sequestration and (2) progress of microbial activity during enhanced oil recovery. Furthermore, our work suggests the possibility of applying electrical measurements to investigations of life on other planets.

References

Abdel Aal, G. Z., E. A. Atekwana, L. D. Slater, and E. A. Atekwana (2004), Effects of microbial processes on electrolytic and interfacial electrical properties of unconsolidated sediments, *Geophys. Res. Lett.*, *31*(12), L12505 doi:10.1029/2004GL020030.

Atekwana, E. A., E. A. Atekwana, D. D. Werkema, J. P. Allen, L. A. Smart, J. W. Duris, D. P. Cassidy, W. A. Sauck, and S. Rossbach (2004), Evidence for microbial enhanced electrical conductivity in hydrocarbon-contaminated sediments, *Geophys. Res. Lett.*, *31*, L23501, doi:10.1029/2004GL021359.

Bunthof, C. J., S. van Schalkwijk, W. Meijer, T. Abee, and J. Hugenholtz (2001), Fluorescent method for monitoring cheese starter permeabilization and lysis, *Appl. Environ. Microbiol.*, *67*, 4264–4271.

Gorby, Y. A., et al. (2006), Electrically conductive bacterial nanowires produced by Shewanella oneidensis strain MR-1 and other microorganisms, *Proc. Natl. Acad. Sci. USA*, *103*(30), 11,358–11,363.

Lehman, M. R., F. S. Colwell, and G. A. Bala (2001), Attached and unattached microbial communities in a simulated basalt aquifer under fracture- and porous-flow conditions, *Appl. Environ. Microbiol.*, *67*(6), 2799–2809.

Mai-Prochnow, A., F. Evans, D. Dalisay-Saludes, S. Stelzer, S. Egan, S. James, J. S. Webb, and S. Kjelleberg (2004), Biofilm development and cell death in the marine bacterium Pseudoaltermonas tunicate, *Appl. Environ. Microbiol.*, *70*, 3232–3238.

Naudet, V., and A. Revil (2005), A sandbox experiment to investigate bacteria-mediated redox processes on self-potential signals, *Geophys. Res. Lett.*, *32*, L11405, doi:10.1029/2005GL022735.

Ntarlagiannis, D., K. H. Williams, L. Slater, and S. Hubbard (2005a), The low frequency electrical response to microbially induced sulfide precipitation, *J. Geophys. Res.*, *110*, G02009, doi:10.1029/2005JG000024.

Ntarlagiannis, D., N. Yee, and L. Slater (2005b), On the low frequency induced polarization of bacterial cells in sands, *Geophys. Res. Lett.*, *32*, L24402, doi:10.1029/2005GL024751.

Reguera, G., K. D. McCarthy, T. Mehta, J. S. Nicoll, M. T. Tuominen, and D. R. Lovely (2005), Extracellular electron transfer via microbial nanowires, *Nature*, *435*(23), 1098–1101.

Silverman, M. P., and E. F. Munoz (1974), Microbial metabolism and dynamic changes in the electrical conductivity of soil solutions: A method for detecting extraterrestrial life, *Appl. Microbiol.*, *28*(6), 960–967.

Slater, L., and D. P. Lesmes (2002), IP interpretation in environmental investigations, *Geophysics*, *67*, 77–88.

Vanhala, H., and H. Soininen (1995), Laboratory technique for measurement of spectral induced polarization response of soil samples, *Geophys. Prospect.*, *43*, 655–676.

Watnick, P., and R. Kolter (2000), Biofilm, city of microbes, *J. Bacteriol.*, *182*(10), 2675–2679.

Williams, K. H., D. Ntarlagiannis, L. Slater, A. Dohnalkova, S. S. Hubbard, and J. f. Banfield (2005), Geophysical imaging of stimulated microbial biomineralization, *Environ. Sci. Technol.*, *39*(19), 7592–7600.

————————————

E. Atekwana and E. Atekwana, Boone Pickens School of Geology, Oklahoma State University, 105 Noble Research Center, Stillwater, OK 74078, USA. (estella.atekwana@okstate.edu)

C. A. Davis, Department of Geological Sciences and Engineering, University of Missouri-Rolla, 1870 Miner Circle, Rolla, MO 65409, USA.

M. R. Mormile, Department of Biological Sciences, University of Missouri-Rolla, 1870 Miner Circle, Rolla, MO 65409, USA.

S. Rossbach, Department of Biological Sciences, Western Michigan University, 1903 W. Michigan Avenue, Kalamazoo, MI 49008, USA.

L. D. Slater, Department of Earth and Environmental Sciences, Rutgers University, 195 University Avenue, Newark, NJ 07102, USA.